

# Preconditioning-induced CXCL12 upregulation minimizes leukocyte infiltration after stroke in ischemia-tolerant mice

Uma Maheswari Selvaraj<sup>1</sup>, Sterling B Ortega<sup>1</sup>, Ruilong Hu<sup>2</sup>, Robert Gilchrist<sup>2</sup>, Xiangmei Kong<sup>1</sup>, Alexander Partin<sup>1</sup>, Erik J Plautz<sup>1</sup>, Robyn S Klein<sup>4</sup>, Jeffrey M Gidday<sup>2,3,\*</sup> and Ann M Stowe<sup>1,\*</sup>

## Abstract

Repetitive hypoxic preconditioning creates long-lasting, endogenous protection in a mouse model of stroke, characterized by reductions in leukocyte–endothelial adherence, inflammation, and infarct volumes. The constitutively expressed chemokine CXCL12 can be upregulated by hypoxia and limits leukocyte entry into brain parenchyma during central nervous system inflammatory autoimmune disease. We therefore hypothesized that the sustained tolerance to stroke induced by repetitive hypoxic preconditioning is mediated, in part, by long-term CXCL12 upregulation at the blood–brain barrier (BBB). In male Swiss Webster mice, repetitive hypoxic preconditioning elevated cortical CXCL12 protein levels, and the number of cortical CXCL12+ microvessels, for at least two weeks after the last hypoxic exposure. Repetitive hypoxic preconditioning-treated mice maintained more CXCL12-positive vessels than untreated controls following transient focal stroke, despite cortical decreases in CXCL12 mRNA and protein. Continuous administration of the CXCL12 receptor (CXCR4) antagonist AMD3100 for two weeks following repetitive hypoxic preconditioning countered the increase in CXCL12-positive microvessels, both prior to and following stroke. AMD3100 blocked the protective post-stroke reductions in leukocyte diapedesis, including macrophages and NK cells, and blocked the protective effect of repetitive hypoxic preconditioning on lesion volume, but had no effect on blood–brain barrier dysfunction. These data suggest that CXCL12 upregulation prior to stroke onset, and its actions following stroke, contribute to the endogenous, anti-inflammatory phenotype induced by repetitive hypoxic preconditioning.

## Keywords

AMD3100, CXCR4, chemokine, hypoxic preconditioning, stroke

Received 11 May 2015; Revised 5 January 2016; Accepted 8 January 2016

## Introduction

The infiltration of leukocytes into brain parenchyma following stroke is a well-established and predominantly injurious immune response that contributes to blood–brain barrier (BBB) disruption and infarct progression.<sup>1–3</sup> The post-stroke infiltration of immune cells into central nervous system (CNS) includes both the innate (e.g. neutrophils, macrophages) and subsequently the adaptive (e.g. T and B cells) immune systems.<sup>2</sup> The diapedesis of leukocytes into the ischemic hemisphere is orchestrated by a variety of leukocyte and endothelial cell adhesion molecules, as well as several chemokines.<sup>4,5</sup> Chemokine (C-X-C motif) ligand 12 (CXCL12), when displayed on the abluminal

<sup>1</sup>Department of Neurology & Neurotherapeutics, UT Southwestern Medical Center, Dallas, TX, USA

<sup>2</sup>Department of Neurological Surgery, Washington University School of Medicine, St. Louis, MO, USA

<sup>3</sup>Department of Ophthalmology, Louisiana State University School of Medicine, New Orleans, LA, USA

<sup>4</sup>Department of Medicine, Washington University, St Louis, MO, USA

\*Co-senior authors

### Corresponding author:

Ann M Stowe, Department of Neurology and Neurotherapeutics, UT Southwestern Medical Center, 6000 Harry Hines Blvd, MC8813 Dallas, TX 75390, USA.

Email: Ann.Stowe@utsouthwestern.edu

surface of cerebral microvessels,<sup>6,7</sup> plays an important role in CNS immune privilege. In that location, CXCL12 maintains a physical coupling between astrocyte end-feet and endothelial barrier proteins<sup>6</sup> to “trap” and prevent the migration of leukocytes expressing the CXCL12 receptor, chemokine (C-X-C motif) receptor 4 (CXCR4), into brain parenchyma.<sup>7</sup> During autoimmune inflammation, CXCR7 within endothelial cells internalizes abluminal CXCL12, allowing CXCR4-expressing leukocytes to transmigrate past the BBB and into parenchymal CNS, where they can inflict damage.<sup>7,8</sup>

Accumulating preclinical evidence indicates that neurovascular injury following stroke can be dramatically attenuated by inducing a transient, ischemia-resistant state prior to stroke upon exposure to a non-injurious “preconditioning” stimulus.<sup>9</sup> We recently developed a mouse model of repetitive hypoxic preconditioning (RHP) that promotes a uniquely long-lasting, ischemia-tolerant phenotype that is sustained for months following the end of treatment.<sup>10</sup> In mice subjected to stroke two or four weeks after the last RHP treatment, acute leukocyte diapedesis into the ischemic hemisphere was minimized,<sup>11</sup> as was BBB permeability,<sup>10</sup> which promotes endogenous protection as both of these events contribute to neuronal injury.<sup>1,2</sup> Given the role of CXCL12 in regulating leukocyte diapedesis across the BBB,<sup>7</sup> and that CXCL12 is one of two chemokines under the transcriptional regulation of hypoxia-inducible factor (HIF)-1 $\alpha$ ,<sup>12</sup> we undertook a series of studies to test the hypothesis that CXCL12 contributes to the RHP-induced ischemia-tolerant phenotype. We provide evidence of a sustained upregulation of CXCL12 protein in response to RHP, and an increase in the number of cortical microvessels expressing this chemokine abluminally both prior to and following focal stroke. Continuous administration of the CXCR4 antagonist AMD3100 for two weeks following RHP abrogated the RHP-mediated, pre-stroke increase in the number of CXCL12<sup>+</sup> microvessels, as well as the RHP-mediated post-stroke reduction in leukocyte diapedesis into the ischemic hemisphere. Specifically, AMD3100 treatment led to elevated populations of B cells, activated macrophages, and NK cells in the ischemic cortex, concomitant with elevated lesion volume despite prior preconditioning. Taken together, our findings support a CXCL12-mediated, anti-inflammatory mechanism as causal to long-term RHP-induced neurovascular protection.

## Materials and methods

### *RHP and transient focal stroke*

Washington University in St. Louis and UT Southwestern Medical Center approved all procedures

according to AAALAC accreditation and current PHS Animal Welfare Assurance requirements for the respective institutions. Animal reporting is according to ARRIVE guidelines. Adult male Swiss-Webster mice were purchased (Harlan) at six to seven weeks old at start of experiments, and randomly assigned to either RHP or control groups. Home cages with standard cob bedding were placed in hypoxic chambers to induce RHP.<sup>10</sup> RHP is defined by nine stochastic exposures to hypoxia (8% or 11% O<sub>2</sub>; 2 h or 4 h) over a two-week period.<sup>10</sup> Control animals were placed in identical chambers for the same duration but exposed to 21% O<sub>2</sub> (i.e. room air). RHP/room air exposure was initiated at the same time of day for each exposure, and animals were otherwise housed in standard animal housing, with a 12/12 light cycle, and food and water ad libitum.

Stroke was induced two weeks following the end of RHP by surgeons blinded to condition, between 8:00 and 14:00 h, with 10 mice/surgeon/day maximum, with minimum of duplicate experimental days for each outcome measure. Pre-operative weight did not vary between control (35  $\pm$  2 g) and treated (37  $\pm$  2 g) groups. An intraluminal suture was placed to impede blood flow to the middle cerebral artery (MCA) in anesthetized animals (1.8–2% isoflurane/ 70% NO<sub>2</sub>/ 30% O<sub>2</sub>), while body temperature was maintained at 37°C.<sup>10</sup> Transcranial laser Doppler flowmetry (TSI, Inc.; St. Paul, MN, USA) confirmed the occlusion (>80% reduction of MCA blood flow relative to baseline). Animals were placed in an incubator (34°C) during the 60-min period of ischemia, and then re-anesthetized to withdraw the intraluminal suture. Flowmetry confirmed MCA reperfusion (return of blood flow to >50% of baseline) and animals were monitored until recovered, and daily thereafter while remaining in standard cage housing with moistened chow available. Mice not meeting the above MCA occlusion and reperfusion criteria were excluded from further analysis at the time of surgery. This included 29 out of 155 mice for post-stroke chemokine and histology studies, flow cytometry analysis, and EB/TTC studies. Additional pre- and post-stroke brain lysates in Figure 1(d) were collected during previously reported experiments,<sup>11</sup> though the CXCL12 analysis is new for this paper. Therefore, those animals are not included in these exclusion numbers.

### *Pharmacologic blockade of CXCR4 with continuous AMD3100 administration*

Four hours after the final RHP exposure that began at 8:00 a.m., animals were anesthetized (1.8–2% isoflurane/ 70% NO<sub>2</sub>/ 30% O<sub>2</sub>), a small incision on the lateral thoracic wall made, and an osmotic mini-pump

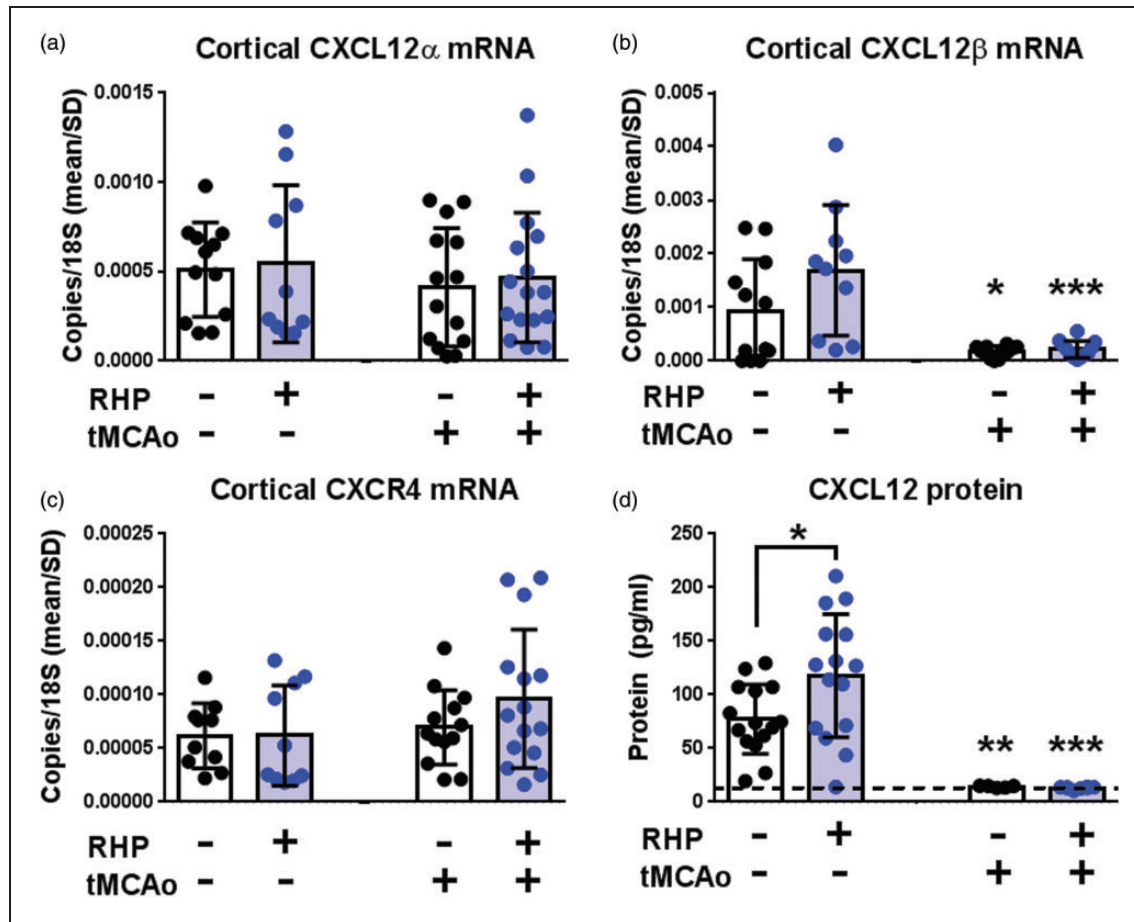


**Figure 1.** RHP upregulates CXCL12 protein prior to stroke, with minimal effect following stroke. (a–c) Cortical (b) CXCL12 $\beta$  mRNA, but not (a) CXCL12 $\alpha$  and (c) CXCR4 mRNA, was mildly increased at two weeks following the end of RHP ( $n = 10$ ; blue circles) compared to naïve controls ( $n = 12$ ; black circles). One day following tMCAo, CXCL12 $\beta$  mRNA, but not CXCL12 $\alpha$  or CXCR4, is downregulated in both groups ( $n = 14$ – $16$ /group). (d) RHP increased pre-stroke CXCL12 protein ( $n = 15$ /group) that, like mRNA, exhibited a downregulation following tMCAo ( $n = 5$ – $8$ /group). Values are shown as mean  $\pm$  standard deviation (SD), with \* $p < 0.05$ , \*\* $p < 0.01$ , \*\*\* $p < 0.001$  versus untreated or RHP-treated pre-stroke expression unless otherwise indicated.

(Alzet; Cupertino, CA, USA) placed subcutaneously until sacrifice. Animals were randomized to receive mini-pumps filled with either AMD3100 (20 mg/ml in sterile PBS; Sigma-Aldrich; St. Louis, MO, USA), a bicyclam strictly confined as an antagonist of CXCR4 signaling,<sup>13</sup> or sterile phosphate-buffered saline (PBS) vehicle. The pumps provided continuous administration at an infusion rate of 0.5  $\mu$ l/h for two weeks following completion of RHP.<sup>7</sup>

#### Quantification of mRNA and protein

Animals were sacrificed with isoflurane overdose, transcardially perfused (20 ml 0.01 M PBS) and brains dissected and snap-frozen in liquid nitrogen. Cortical tissues were homogenized in PureZOL (Bio-Rad; Hercules, CA), RNA isolated with Aurum total RNA kit (Bio-Rad), and cDNA generated with iScript cDNA

Synthesis Kit (Bio-Rad). CXCL12 $\alpha$  (Forward: TTC CGC TTC TCA CCT CTG TAG C; Reverse: CAA GTG AGA GGA AAG CAA AGG G), CXCL12 $\beta$  (Forward: GTG AGG CCA GGG AAG AGT GA; Reverse: AGA CAG AAT GAT GAG CAT GGT GG) and CXCR4 (Forward: TTG GCC TTT GAC TGT TGG TG; Reverse: TTG GCC TTT GAC TGT TGG TG) mRNA (Integrated DNA Technologies; Coralville, IA, USA) levels were normalized against ribosomal 18S (Forward: GTA ACC CGT TGA ACC CCA TT; Reverse: CCA TCC AAT CGG TAG TAG CG).<sup>10</sup> Data were quantified on a 7500 Real Time PCR System (Life Technologies). Brain lysates were collected during cortical processing for quantification of CXCL12 protein levels. The quantitative immunoassay of CXCL12 was performed with standard ELISA kits (R&D Systems) according to the manufacturer's instructions.<sup>11</sup>

### Flow cytometry

Animals were sacrificed with isoflurane overdose two days after tMCAo and transcardially perfused with 30 ml 0.01 M PBS prior to brain dissection.<sup>11</sup> At the time of perfusion, all animals cleared visible blood from the contralateral hemisphere and sinuses and were included in the experiments. The cerebellum was removed, with the remaining hemispheres divided at the midline and processed through a 70  $\mu$ m mesh strainer, including the leptomeninges. Dissociated hemispheres were washed in HyClone RPMI (Thermo Scientific; Waltham, MA, USA), and lymphocytes isolated with a 70:30 discontinuous Percoll gradient. Cells were resuspended (1 ml RPMI) and hemocytometer counts collected for each sample. Non-specific binding was blocked (FcR $\gamma$ II/III; BD Biosciences) and leukocytes identified by antibodies for general leukocytes (CD45-APC-Cy7), B cells (CD19-Alexa 700), monocytes/macrophages (CD11b-PE), neutrophils (GR1-FITC), NK cells (NK1.1-Percp 5.5), and T cells (TCR-PE-Cy5; CD4-PacBlue). After incubation, cells were washed with FACS wash buffer (PBS with 1% BSA, 0.22  $\mu$ m filtered) and fixed (1% paraformaldehyde). All samples were run on a BD-FACS Aria flow cytometer using FACS Diva 6.0 software and data analyzed using FlowJo (Tree Star Inc.; Ashland, OR, USA). Hemocytometer counts were used to quantify absolute number.

### Histology and confocal CXCL12 localization analysis

Animals were sacrificed with isoflurane overdose, transcardially perfused (20 ml 0.01 M PBS, 40 ml 4% paraformaldehyde) and brains removed for cryoprotection (30% sucrose in PBS). Frozen coronal sections were prepared, blocked, and stained using standard procedures.<sup>7</sup> Primary antibodies and dilutions were: CXCL12 (1:20; PeproTech; Rocky Hill, NJ, USA), and CD31 for endothelial cells (1:50; BD Biosciences; San Jose, CA, USA). Primary antibodies were detected using Alexa Fluor 488, or 594 (1:400; Invitrogen; Grand Island, NY, USA) and nuclei were counterstained with ToPro3 or DAPI (Life Technologies). Images were obtained using a confocal laser-scanning microscope (Olympus FV-500; Center Valley, PA or Zeiss LSM 780; Thornwood NY, USA). Quantification of CXCL12 fluorescence within and around microvessels was performed as previously described using Fluoview software (Olympus).<sup>7</sup> Briefly, five images were taken of the left cortical hemisphere from adjacent coronal sections from each of the anterior, medial, and posterior portions of the MCA territory. Images were blinded for analysis. A line was drawn perpendicular to the length of each microvessel – identified by CD31 fluorescence –

and within an area of CXCL12 expression if the vessel also colocalized with CXCL12 (Figure 2). Fluoview quantified fluorescence intensity for each wavelength along the length of the drawn line, and both peak and background intensities from a space without positive immunofluorescence were recorded. If the vessel was in cross-section to the coronal plane (Figure 2(a)), both sides of the vascular wall were quantified independently. Separate groups of naïve mice were analyzed in conjunction with the AMD3100- and PBS-treated animals to control for inter-experiment variability in confocal image acquisition between microscopes and quantification methods between observers.

### Statistics

Technicians blinded to experimental condition performed all analyses. Outliers were identified using ROUT (Prism) from a Gaussian distribution with a  $Q=1$ . This resulted in eight total outliers identified for all data sets, which removed six from the qPCR studies and two from the EB/TTC cohorts. All between-group differences were analyzed using Student's t-test, or by one-way ANOVA with Sidak post-hoc analysis (GraphPad Prism, version 6). Post-hoc power analysis confirmed adequate "n" for all cohorts except the qPCR data (Figure 1), which would require an  $n=27$ /group to confirm differences between groups. All values in text and graphs are mean  $\pm$  standard deviation (SD). Significance was accepted as  $p < 0.05$ .

## Results

### RHP upregulates cortical CXCL12 mRNA and protein prior to stroke

The promoter region of the CXCL12 gene contains a HIF-1 $\alpha$  binding sequence for the hypoxia-dependent regulation of both the CXCL12 $\alpha$  and CXCL12 $\beta$  alternatively spliced isoforms,<sup>12</sup> as does the promoter region of the gene for the CXCL12 receptor CXCR4.<sup>14</sup> Therefore, we first sought to determine the effects of our RHP intervention on CXCL12 and CXCR4 expression in the healthy CNS. Although cortical CXCL12 $\alpha$  mRNA was unaffected (Figure 1(a)), CXCL12 $\beta$  mRNA remained doubled, although non-significantly (Figure 1(b)), two weeks after RHP, a time point associated with the most robust neurovascular protection against transient focal stroke.<sup>10</sup> However, cortical CXCL12 protein levels, which reflect both CXCL12 $\alpha$  and CXCL12 $\beta$  mRNA products, were elevated after RHP ( $p < 0.05$ ; Figure 1(d)). The mRNA expression for CXCR4 was unaffected by RHP (Figure 1(c)). Thus, RHP promotes a persistent upregulation in

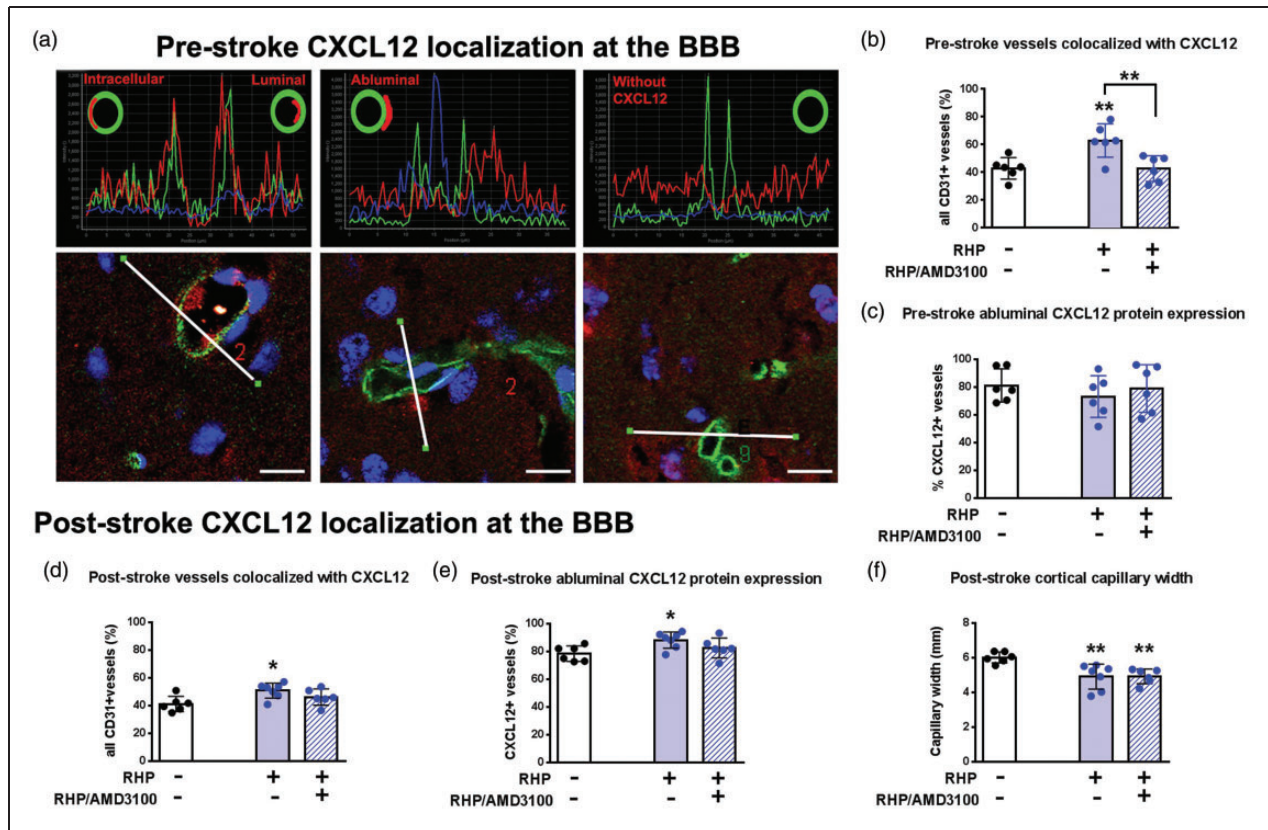


**Figure 2.** RHP increases the number of vessels exhibiting abluminal CXCL12 both prior to and after stroke. (a) Photomicrographs from a naïve animal, with CXCL12 (red) and microvessels (CD31; green) shown. White lines (lower panels) denote the lengths analyzed across the tissue that are represented by the respective fluorescent intensity plots (upper panels). Pictorial cross-sections in upper panels show intracellular (within the endothelial cell), luminal (within the vessel), abluminal (outside the vessel, within the parenchyma), and “no CXCL12” expression profiles. Scale bar=10 $\mu$ m. (b) Repetitive hypoxic preconditioning (RHP; solid blue bar; n=6) increased the number of CXCL12<sup>+</sup> microvessels compared to naïve brain (white bar; n=6) two weeks following the end of RHP. In the presence of the CXCR4 antagonist AMD3100, the effect of RHP on microvascular CXCL12 expression was reversed (hatched bar; n=6), but did not affect abluminal localization (c). (d) tMCAo (white bar; n=6) did not change the number of cortical microvessels expressing CXCL12 protein versus baseline cortex or (e) the number of vessels with abluminal localization. However, prior RHP treatment (blue bars; n=7) increased the number of CXCL12-expressing microvessels with abluminal localization, effects attenuated by AMD3100 (hatched bar; n=6). (f) Both RHP-treated cohorts had reduced capillary dilation compared to the post-stroke controls. Values are shown as mean  $\pm$  standard deviation (SD). \* $p < 0.05$ , \*\* $p < 0.01$  versus untreated, naïve or stroke control condition.

cortical CXCL12 protein expression through two weeks after the last hypoxic exposure.

### RHP increases the number of CXCL12-positive microvessels prior to stroke

Previous investigations of CXCL12 during multiple sclerosis in human tissue and mouse models revealed that abluminally-distributed (i.e. outside but adjacent to the microvessel; Figure 2(a)) CXCL12 normally serves to prevent diapedesis of CXCR4-expressing leukocytes into CNS parenchyma, but that, with advancing pathology, CXCL12 becomes redistributed from abluminal to luminal spaces, thereby allowing

leukocyte egress into tissue.<sup>4,7</sup> To more closely examine how RHP might affect microvessel-associated CXCL12 protein expression and topology, we quantified the percentage of cortical microvessels with abluminal, intracellular, and luminal localization of CXCL12 in naïve and RHP-treated mice, before and after stroke. Under naïve conditions, 43% (177/413) of all CD31<sup>+</sup> microvessels colocalized with CXCL12 protein (i.e. were CXCL12-positive; Figure 2; Table 1). Two weeks after RHP (but prior to stroke), a significant increase (to 62% [219/352];  $p < 0.01$ ) was noted in the percentage of microvessels that were CXCL12<sup>+</sup>. However, RHP did not increase the number of microvessels exhibiting an abluminal localization profile for

**Table 1.** Quantification of abluminal CXCL12 expression in cortical vessels following RHP.

Condition	Total vessels analyzed	CXCL12+ vessels	Vessels with abluminal CXCL12	Vessels with intracellular CXCL12	Vessel diameter (avg, micron)
Naïve	117	51	36	15	4.29
	59	32	22	10	5.81
	64	28	22	6	5.54
	51	23	22	1	4.98
	59	18	14	4	3.3
	63	25	24	1	3.54
RHP-treated	59	46	29	17	4.97
	65	40	32	8	5.75
	58	41	34	7	6.91
	51	32	22	10	4.12
	69	29	27	2	4.52
	50	31	16	15	4.14
RHP + AMD3100	57	28	16	12	3.67
	54	28	21	7	3.83
	52	26	16	10	3.27
	61	25	24	1	5.71
	62	19	18	1	6.11
	61	20	18	2	5.6
Control tMCAo	71	28	23	5	6.37
	63	22	16	6	5.83
	67	28	24	4	5.94
	53	20	15	5	6.37
	55	28	23	5	5.55
	61	26	19	7	6.06
RHP + tMCAo	67	36	28	8	3.79
	66	35	32	3	4.91
	63	34	30	4	4.03
	48	24	20	4	5.35
	55	26	24	2	5.51
	44	18	17	1	5.22
RHP + AMD3100 + tMCAO	70	40	36	4	5.57
	61	28	24	4	4.23
	69	37	30	6	5.26
	62	28	20	8	4.68
	67	30	28	2	4.86
	55	28	23	5	5.32
	60	22	18	4	5.22

RHP: repetitive hypoxic preconditioning; wks: weeks; AMD: AMD3100; PBS: phosphate-buffered saline; tMCAo: transient middle cerebral artery occlusion; avg: average.

CXCL12 (79% [140/177] in naïve mice vs. 73% [160/219] in RHP-treated mice). In the remaining CXCL12<sup>+</sup> vessels, CXCL12 was localized intracellularly. Treating mice continuously after RHP with AMD3100, a small-molecule antagonist of CXCR4, attenuated the RHP-induced increase in the number of CXCL12<sup>+</sup>/CD31<sup>+</sup> microvessels (42% [146/347];  $p < 0.01$  vs. RHP;

Figure 2(b)). AMD3100 treatment did not affect proportion of vessels with abluminally localized CXCL12 (Figure 2(c)). These findings indicate that CXCL12-CXCR4 signaling in response to RHP drives increases in the number of CXCL12<sup>+</sup> microvessels, but does not significantly affect CXCL12 polarity, prior to stroke.

### **Prior RHP minimally affects post-ischemic CXCL12 expression**

CXCL12 $\beta$  mRNA expression levels decrease between 6 h and four days following permanent focal stroke,<sup>15</sup> which was postulated to be a protective mechanism on the part of the cortical vasculature to minimize adherence and diapedesis of circulating CXCR4-expressing leukocytes activated during ischemia. This hypothesis was confirmed by blocking CXCL12-CXCR4 signaling with AMD3100 beginning two days after stroke, which reduced the extent of leukocyte infiltration and improved functional recovery.<sup>16,17</sup> Given that RHP also results in reduced leukocyte diapedesis at one and two days after transient focal stroke,<sup>10,11</sup> we sought to determine whether this phenotype was secondary to an RHP-mediated reduction in post-stroke CXCL12 expression. Stroke reduced CXCL12 $\beta$  mRNA one day later in both untreated ( $p < 0.05$ ) and RHP-treated ( $p < 0.001$ ) mice compared to pre-stroke values (Figure 1(b)). Stroke had no effect on CXCL12 $\alpha$  or CXCR4 mRNA expression in either group. The global reductions in post-stroke CXCL12 $\beta$  message preceded reductions in cortical CXCL12 protein expression two days after stroke for both untreated ( $p < 0.01$ ) and RHP-treated ( $p < 0.001$ ) mice relative to pre-stroke values (Figure 1(d)). In fact, the RHP-induced upregulation of CXCL12 protein was not sustained two days post-stroke, although values for cortical CXCL12 in both cohorts were at the lower limit of detection for the protein assay.

### **Increases in CXCL12<sup>+</sup> vessel numbers, but not altered polarity, correlate with reductions in post-stroke leukocyte diapedesis**

Given that both untreated and RHP-treated mice exhibited reductions in CXCL12 message and protein expression in the ischemic hemisphere following stroke, we then sought to determine the effect of stroke on CXCL12<sup>+</sup> microvessel number and on CXCL12 polarity in both groups. In untreated mice, stroke did not significantly affect the number of CXCL12<sup>+</sup> microvessels (41% (152/370) of all CD31<sup>+</sup> microvessels; Figure 2(d); Table 1), nor did it lead to a significant redistribution of abluminal CXCL12 (Figure 2(e)) to either the intracellular or luminal compartments (data not shown). RHP-treated mice maintained post-stroke CXCL12<sup>+</sup> expression in 52% of the microvessels (213/413), significantly elevated relative to both pre-stroke ( $p < 0.05$ ) and untreated post-stroke ( $p < 0.05$ ) cohorts. RHP also enhanced the percentage of CXCL12<sup>+</sup> microvessels with abluminal localization (78% [120/152] in control mice vs. 88% [187/213] in RHP-treated mice;  $p < 0.05$ ). As with the pre-stroke values, treating mice

continuously with AMD3100 after RHP countered the RHP-induced increase in the both the number of CXCL12<sup>+</sup>/CD31<sup>+</sup> post-stroke microvessels (46% [173/374]), as well as the enhanced abluminal localization of CXCL12 in the preconditioned cortex (83% [143/173]). Interestingly, stroke induced a dilation of capillaries in control mice following stroke ( $4.5 \pm 0.42 \mu\text{m}$  in naïve mice vs.  $6.0 \pm 0.13 \mu\text{m}$  in control stroke mice;  $p < 0.01$ ; Table 1). Both RHP-treated cohorts, however, exhibited reductions in capillary width compared to post-stroke control mice (PBS:  $4.9 \pm 0.72 \mu\text{m}$  and AMD:  $4.9 \pm 0.17 \mu\text{m}$ ; both  $p < 0.01$ ; Figure 2(f)). These results are consistent with the hypothesis that leukocyte diapedesis into ischemic cortex is not the result of an active translocation of CXCL12 from an abluminal location to either a luminal or intracellular location, as occurs during CNS autoimmune disease.<sup>8</sup> That RHP-mediated reductions in post-ischemic leukocyte diapedesis occur independently of changes in CXCL12 polarity suggests that absolute expression levels of CXCL12 on cerebral microvessels may instead regulate leukocyte diapedesis.

### **Long-term CXCR4 antagonism following RHP increases leukocyte diapedesis into the ischemic hemisphere and exacerbates infarction**

Our findings that RHP upregulates CXCL12 for weeks prior to stroke, and increases the number of CXCL12<sup>+</sup> vessels following stroke, seemingly contradict reports that blockade of post-stroke CXCL12 expression is beneficial.<sup>16–18</sup> We thus sought causal evidence for enhanced CXCL12-CXCR4 signaling in the RHP-induced, post-stroke anti-inflammatory phenotype we observed.<sup>10,11</sup> Two separate cohorts of RHP-treated mice were used: An experimental group that received AMD3100 after the completion of RHP, and a control group that received PBS vehicle after RHP. We quantified cortical leukocyte diapedesis by flow cytometry (Supplemental Figure 1) two days following focal stroke in both AMD3100-treated, and PBS-treated mice with prior RHP. Consistent with our previous study,<sup>11</sup> in mice receiving PBS vehicle, ischemia-induced increases in CD45<sup>+</sup> leukocyte diapedesis were abrogated by prior RHP, with leukocyte populations in the ischemic hemisphere indistinguishable from levels in the contralateral, uninjured cortex (Figure 3(a)). All specific leukocyte subpopulations (i.e. B cells, CD8 T cells, macrophages, neutrophils, myeloid cells, and NK cells) were not elevated over contralateral cortex, with the exception of CD4<sup>+</sup> T cells ( $p < 0.0001$  vs. contralateral hemisphere; Figure 4(c)).

However, in mice treated with AMD3100 following RHP, this RHP-induced suppression of CD45<sup>+</sup> leukocyte diapedesis was lost resulting in a significant egress

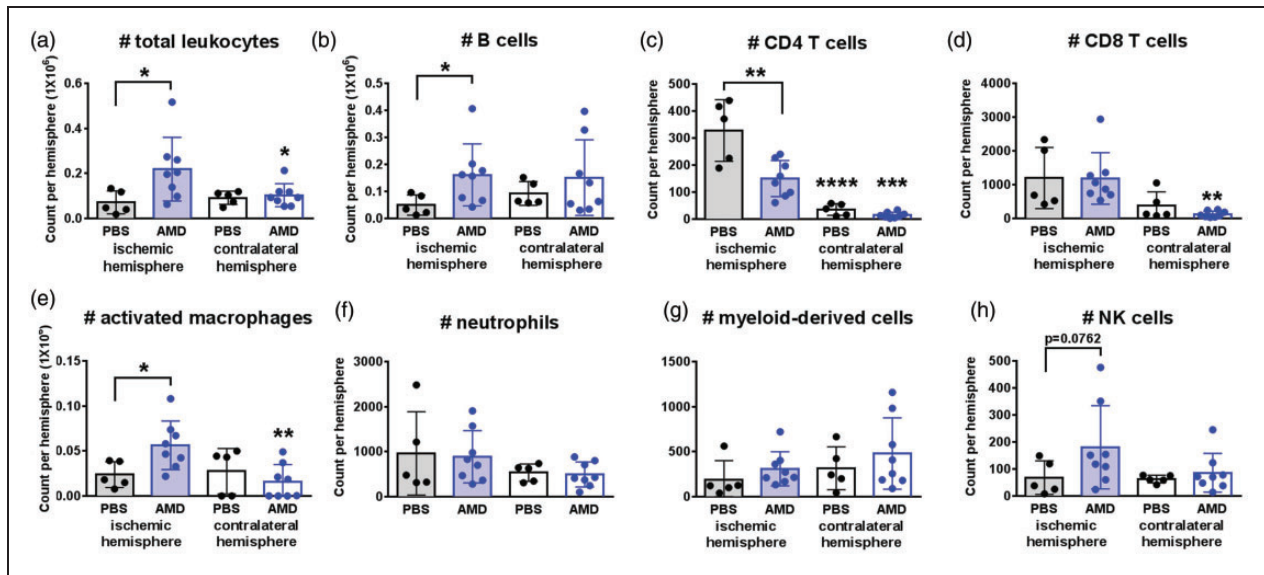


**Figure 3.** AMD3100 blocks the protective effects of RHP on post-stroke leukocyte diapedesis. (a–h) Overall leukocyte diapedesis was diminished in the ischemic cortex of RHP-treated mice with PBS ( $n = 5$ ; black circles, shaded bars) to levels indistinguishable from the contralateral, uninjured cortex (black circles, white bars). Only the CD4 T cell populations were elevated over contralateral cortex in RHP/PBS controls. AMD3100- (AMD;  $n = 8$ ) treated mice exhibited increased B cell, activated macrophage, and NK cell diapedesis in the ischemic hemisphere (blue circles, shaded bars) compared to contralateral cortex (blue circles, white bars) with the exception of a suppressed (c) CD4<sup>+</sup> T cell diapedesis. Values are shown as mean  $\pm$  standard deviation (SD). \* $p < 0.05$ , \*\* $p < 0.01$ , \*\*\* $p < 0.001$ , \*\*\*\* $p < 0.0001$  versus populations in the corresponding ischemic hemisphere unless otherwise indicated.

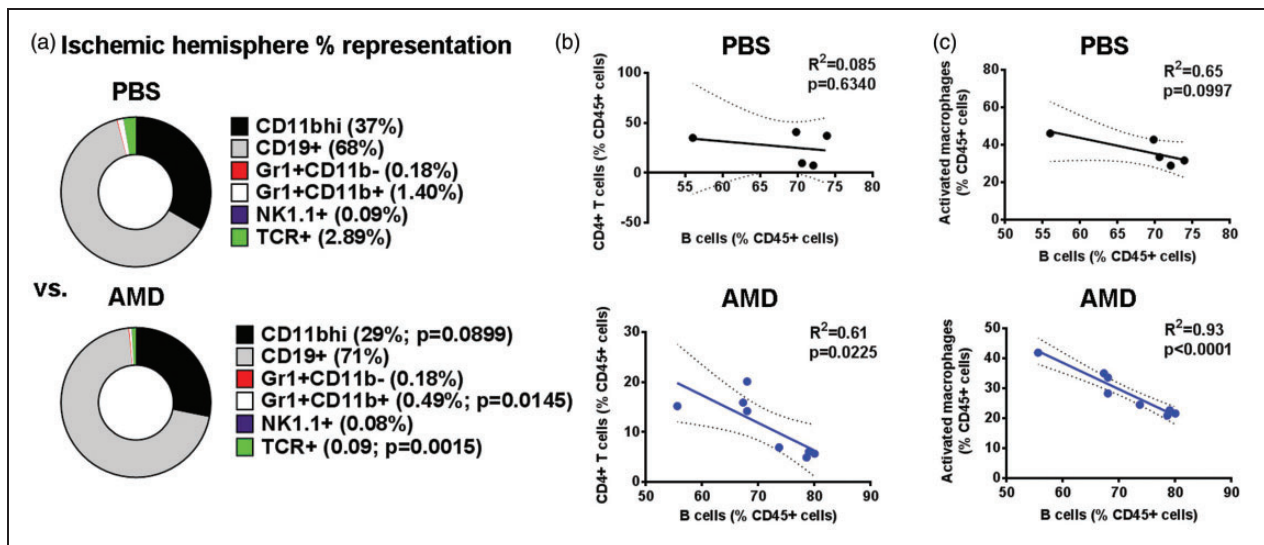


**Figure 4.** B cells in RHP/AMD3100-treated mice inhibit the egress of other immune cells in the ischemic hemisphere. (a) Percent distribution of identified leukocyte subsets from the ischemic hemispheres for PBS- and AMD-treated mice shown in Figure 3. (b, c) In AMD-treated mice (lower panels, blue graph), B cells negatively regulated the presence of both (b) CD4<sup>+</sup> T cells and (c) activated macrophage representations within the ischemic hemisphere, a phenotype not found in PBS-treated mice (upper panels, black graph). Direct  $p$  values are given.

of leukocytes into the ischemic hemisphere when compared to the uninjured cortex ( $p < 0.05$ ; Figure 3(a)) and similar to prior results in untreated controls.<sup>11</sup> Specifically, AMD3100 treatment resulted in increases

in the number of B cells ( $p < 0.05$ ), activated macrophages ( $p < 0.05$ ), and natural killer (NK) cells in the ischemic hemisphere compared to RHP/PBS controls (Figure 3(b), (e) and (h)). In contrast, the previous



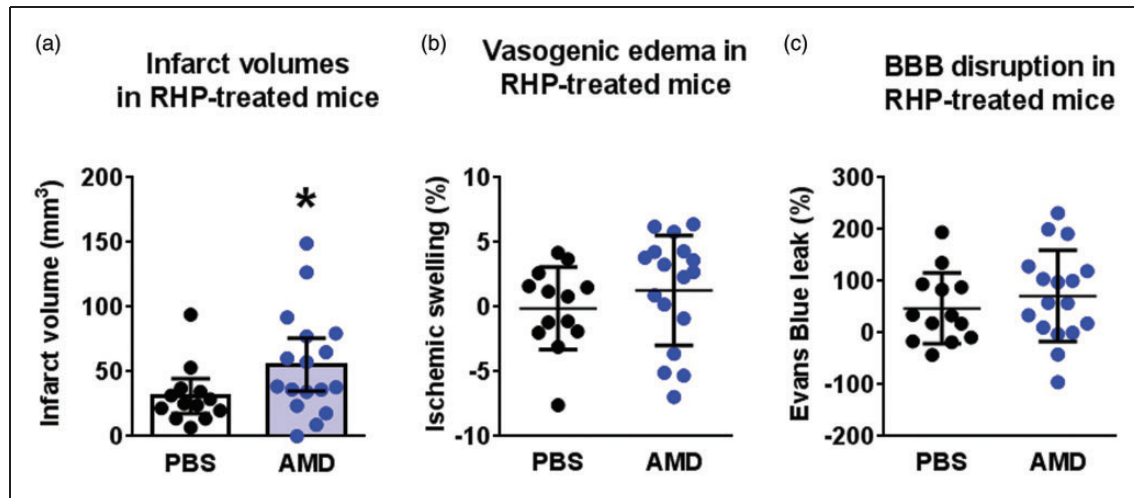


**Figure 5.** CXCL12 signaling is required for RHP-induced reductions in infarct volume. RHP-treated mice receiving AMD3100 (AMD; blue circles;  $n = 17$ ) exhibited (a) larger infarct volumes, but (b) no increase in the extent of ipsilateral edema or (c) Evans blue leak relative to RHP/PBS-treated controls (black circles;  $n = 13$ ). Values are shown as mean  $\pm$  standard deviation (SD). \* $p < 0.05$  versus RHP/PBS-treated controls.

elevation of CD4<sup>+</sup> T cells in the ischemic hemisphere was countered by AMD3100 following RHP ( $p < 0.01$  vs. RHP/PBS control), albeit at levels that remained significantly higher ( $p < 0.001$ ) than those measured in the contralateral hemisphere (Figure 3(c)).

Post-stroke B cell therapy can limit the diapedesis of immune cells during CNS inflammation.<sup>19,20</sup> Furthermore, we recently identified a unique B cell phenotype following RHP (i.e. B<sub>(RHP)</sub> cells) exhibiting enhanced anti-inflammatory mechanisms even prior to CNS injury onset.<sup>11</sup> As AMD3100 treatment resulted in a large influx of B<sub>(RHP)</sub> cells into the ischemic cortex, we sought to determine the influence of these potentially protective B cells on other leukocyte populations. While the overall B cell numbers increased in AMD3100-treated preconditioned mice, the B cell percent distribution within the CD45<sup>+</sup> leukocyte population remained unaffected (RHP/PBS:  $68 \pm 7\%$  vs. RHP/AMD:  $71 \pm 8\%$ ; Figure 4(a)). Linear regression analysis revealed that, in mice receiving AMD3100, higher B<sub>(RHP)</sub> cell populations corresponded to lower populations of CD4<sup>+</sup> T cells ( $R^2 = 0.61$ ;  $p < 0.05$ ; Figure 4(b)) and lower populations of activated macrophages ( $R^2 = 0.93$ ;  $p < 0.0001$ ; Figure 4(c)), but exhibited no association with NK cell or granulocyte populations (data not shown). These inverse relationships were not evidenced in RHP-treated mice without AMD3100, indicating that, with the disruption of CXCL12-CXCR4 signaling in the preconditioned brain that normally suppresses leukocyte diapedesis, B cells remain capable of a secondary immunosuppression when they exist in high numbers in the injured CNS. Post-stroke splenic leukocyte populations in these cohorts (Supplemental Fig. 2) showed no

differences between AMD3100- or PBS-treated mice with RHP. Taken together, these results indicate that CXCL12-CXCR4 signaling is required for the ability of RHP to block the diapedesis of pro-inflammatory leukocytes after stroke.

Leukocyte infiltration, BBB disruption, and neuronal death are not necessarily concomitant events in the ischemic cortex.<sup>21,22</sup> We therefore determined the influence of CXCL12-CXCR4 signaling on infarct progression and BBB disruption in an additional cohort of RHP-treated mice. As shown in Figure 5(a), AMD3100-treated mice receiving RHP exhibited significantly larger ( $p < 0.05$ ) infarct volumes ( $55 \pm 34$  mm<sup>3</sup>) than those measured in their PBS-treated counterparts receiving RHP ( $31 \pm 6$  mm<sup>3</sup>), the latter values consistent with previous results in RHP-treated mice.<sup>10</sup> However, AMD3100-treated mice did not exhibit increases in vasogenic edema, as indexed by ipsilesional hemispheric swelling (Figure 5(b)), and/or enhanced microvascular permeability to Evans blue (Figure 5(c)). These findings indicate that CXCL12-CXCR4 signaling is necessary for the protective effects of RHP, but that this protection occurs independently from any reduction in BBB permeability.

## Discussion

Collectively, our findings indicate that a sustained upregulation of CXCL12 message and protein in response to RHP, manifested as an increased number of CXCL12<sup>+</sup> microvessels, contributes to the long-lasting reduction in post-ischemic leukocyte infiltration observed in preconditioned mice. This conclusion is supported further by the fact that antagonism of

CXCL12/CXCR4 signaling following RHP reversed its protective effects on leukocyte diapedesis, and concomitantly attenuated the extent of RHP-mediated neuroprotection. Our finding that long-term AMD3100 counters endogenous neuroprotection could be considered, at first pass, to be in contrast to previous studies reporting that an acute post-stroke treatment of AMD3100 following either permanent<sup>18</sup> or transient<sup>16,17</sup> focal stroke improved recovery by diminishing infarct volumes, BBB disruption, and inflammation. Ruscher et al.<sup>17</sup> found that AMD3100 administration beginning two days post-stroke limited the diapedesis of T cells, specifically CD4<sup>+</sup> T cells known to contribute to infarct progression,<sup>23</sup> measured four days post-stroke, as well as attenuated microglial activation.<sup>16</sup> We also found this CD4 T cell-specific reduction in our AMD3100 cohort. In our RHP-treated mice, the diapedesis of several other leukocyte subsets,<sup>11</sup> including neutrophils and macrophages, was *naturally* attenuated at the time Ruscher et al.<sup>17</sup> administered AMD3100. Our findings are therefore consonant with the notion that post-stroke AMD3100 recapitulates the protective effect of an RHP-induced downregulation of chemokines, selectins, and integrins, all of which minimize inflammatory mechanisms in the ischemia-tolerant brain, whereas pre-stroke AMD3100 administration to RHP-treated animals blocks the ability of RHP to establish this endogenously protective, anti-inflammatory phenotype.

While the AMD3100-induced reduction in infiltrating CD4 T cells may be a highly cell-selective anti-inflammatory mechanism, our data suggest that, at least in RHP-treated mice, B cells may also contribute to a blockade of CD4 T cell diapedesis. We recently found that only the magnitude of post-ischemic B cell diapedesis was unaffected by RHP, while the extent of diapedesis of all other leukocyte subsets was diminished in the protected ischemic CNS.<sup>11</sup> Moreover, RHP created an anergic regulatory B cell population pre-stroke that could contribute to the anti-inflammatory phenotype. In the current study, long-term AMD3100 treatment prior to stroke enhanced the recruitment and retention of a higher number of B cells in the ischemic hemisphere. The presence of higher B<sub>(RHP)</sub> cells in the ischemic cortex, in turn, significantly limited the diapedesis of CD4<sup>+</sup> T cells and macrophages, but this only effectively diminished overall immune cell numbers for CD4 T cells, not macrophages. This may be a consequence of the different magnitude of cell populations (hundreds vs. thousands, respectively), with smaller CD4 T cell populations more directly influenced by the 100-fold greater B cell populations. These relationships suggest an anti-inflammatory potential for adaptive B<sub>(RHP)</sub> cells in the injured CNS that could be harnessed in future studies

as a potential neurotherapeutic to limit detrimental post-stroke inflammation.

During autoimmune disease, CXCL12 translocates from an abluminal to luminal location that limits the ability of CXCL12 to hold CXCR4-expressing leukocytes in the perivascular space, thus allowing their entry into the CNS parenchyma.<sup>6,7,24</sup> In the present study, we showed that RHP led to a sustained increase in CXCL12 protein deposition along the abluminal surfaces of cerebral microvessels, as evidenced by an increased number of CXCL12<sup>+</sup> microvessels. This “pre-loading” of the BBB with abluminal CXCL12 was maintained in RHP-treated mice after stroke – despite the overall reduction in both CXCL12 message and protein – which, based on the results obtained in AMD3100-treated mice, helped to minimize leukocyte migration into the ischemic cortex. Interestingly, our findings demonstrate that the stroke-induced, sterile inflammatory response within brain parenchyma does not result from a change in CXCL12 polarity to a luminal location. Thus, it would appear that CXCL12-CXCR4 can regulate leukocyte infiltration by more than one mechanism, and which may be dependent on the acute versus chronic inflammatory features of the disease. CXCR7, which mediates the luminal translocation of CXCL12 during CNS autoimmunity,<sup>25</sup> is reduced in the ischemic cortex for a protracted period of time (10 days) after focal stroke in mice,<sup>26</sup> further supporting the notion that CXCL12 translocation from abluminal to luminal locations within the BBB does not participate in acute diapedesis. CXCL12 and CXCR4 are upregulated in a delayed manner following initial post-stroke depletion,<sup>26</sup> coincident with a neuroprotective timeframe for acute AMD3100 administration that limits CD4 T cell diapedesis and improves functional recovery in other studies.<sup>17</sup> In contrast, viral delivery of CXCL12 to the ischemic brain one week after permanent focal stroke reduced long-term cortical atrophy while increasing functional recovery, neurogenesis, and angiogenesis – all of which were blocked with long-term AMD3100 administration.<sup>27</sup> Future studies should therefore investigate how CXCL12-CXCR4 signaling affects the evolution of long-term neurovascular recovery in the CNS, and whether these mechanisms are also modulated by preconditioning or post-conditioning.

Our data suggest that the role of CXCL12 after RHP is largely focused on effects within the BBB. Under physiologic conditions, as well as following permanent focal stroke, CXCL12 $\alpha$  mRNA is expressed by neurons, while CXCL12 $\beta$  mRNA is expressed by cerebral endothelium.<sup>15</sup> Furthermore, the promoter regions of both CXCL12<sup>12</sup> and CXCR4<sup>14</sup> genes contain HIF-1 $\alpha$  binding sequences for hypoxia-dependent regulation. Although the cortical mRNA expression levels of the CXCL12 $\alpha$  isoform, as well as CXCR4, were

unaffected by RHP, the constitutive upregulation of CXCL12 $\beta$  mRNA in the preconditioned cortex and the increase in CXCL12 protein levels are consistent with a long-term upregulation of CXCL12 protein expression in BBB endothelium. A single post-ischemic dose of AMD3100 attenuates post-stroke Evans blue leak and endothelial ZO-1/occludin disassembly,<sup>18</sup> but we found minimal effect of AMD3100 on BBB disruption in RHP-treated mice, which may be due to the already strengthened BBB in preconditioned mice. CXCL12 $\alpha$  increases transendothelial electrical resistance and inhibits vascular permeability through intracellular actin rearrangement, with these phenotypes inhibited by AMD3100.<sup>28</sup> But it is unknown whether CXCL12 $\beta$  can induce similar effects. Given the evidence for BBB disruption and leukocyte diapedesis as independent processes after stroke,<sup>21</sup> future studies should determine the effect of long-term AMD3100 treatment on BBB integrity. We also found that splenic leukocyte subpopulations are unaffected by AMD3100. This indicates that CXCL12 mediates neurovascular protection by decreasing leukocyte diapedesis within the CNS, confirming that regulation of leukocyte infiltration into the ischemic brain is occurring at the BBB and is not reflective of diminished populations within the periphery.

Other studies have provided evidence for CXCL12/CXCR4 signaling in mediating resistance to ischemic injury following conditioning with non-hypoxic stimuli, consistent with a conserved role for this chemokine in establishing cytoprotective phenotypes. For example, CXCL12 plasma levels are elevated for 12–48 h after electroacupuncture preconditioning in mice, as is the post-ischemic expression of CXCL12 in cerebral endothelium.<sup>29</sup> Remote ischemic conditioning in a rat model of myocardial infarction is blocked by AMD3100 and mimicked by direct application of CXCL12.<sup>30</sup> Furthermore, migration of CXCR4-expressing neural stem cells,<sup>31</sup> endothelial progenitor cells (EPCs),<sup>32,33</sup> and bone marrow stromal cells<sup>34</sup> to regions of ischemic injury requires CXCL12/CXCR4 signaling. Our data, taken together with the fact that administration of AMD3100 blocks migration and several metrics of post-stroke recovery,<sup>34,35</sup> may represent facets of a CXCL12-mediated long-term CNS protection. However, the mechanisms by which CXCL12 shifts from mediating long-term endogenous protection to contributing to acute neurovascular injury at later times remain to be determined. CXCL12-recruited EPCs,<sup>32,33</sup> or CXCL12 directly,<sup>27</sup> may also contribute to post-stroke angiogenesis, observations that fit with the clinical finding that serum CXCL12 upregulation after stroke onset significantly correlates with EPC levels and is an independent predictor of reduced infarct volume and better long-term functional

outcome.<sup>36,37</sup> These beneficial contributions of CXCL12 with respect to stem cell migration, angiogenesis, and functional recovery following stroke occur over a post-stroke time frame that is more protracted than the 24–48-h period explored in the current study; future studies to determine the long-term consequences of pre- and post-ischemic CXCL12 upregulation in mice receiving RHP are warranted.

In conclusion, RHP results in a sustained upregulation of CXCL12 in mouse brain. In turn, greater numbers of CXCL12<sup>+</sup> microvessels at the time of stroke may counter ischemia-driven reductions in both CXCL12 message and protein, thereby retaining the ability of CXCL12 to counter mechanisms driving post-ischemic leukocyte diapedesis. In contrast to leukocyte transmigration into CNS parenchyma,<sup>6,7,25</sup> in autoimmune disease that occurs secondary to the microvascular translocation of CXCL12 from abluminal to luminal surfaces, our findings indicate that leukocytes diapedese into the acutely ischemic brain despite the maintenance of abluminal CXCL12. Our results with AMD3100 indicate that the reduction in leukocyte transmigration by RHP still depends on CXCL12, but in a manner related to an increase in the relative number of microvessels expressing this chemokine abluminally, rather than in a polarity-dependent manner. Therefore, the use of neurotherapeutics to enhance and/or expand CXCL12 expression by BBB endothelial cells prior to stroke, either via an engineered CXCL12 analog<sup>38</sup> or viral-mediated delivery,<sup>27,39</sup> could eventually be used in lieu of RHP to create a neuroprotective phenotype in individuals at identified risk for stroke, as well as enhance the recruitment of EPCs to promote cortical angiogenesis prior to injury. Considering the potential long-term use of CXCR4 antagonists in clinical populations,<sup>40</sup> and the efficacy of acute post-stroke antagonism of CXCL12 in animal models,<sup>16–18</sup> it is imperative to continue to probe how CXCL12 contributes to the maintenance of immune privilege during resting, physiologic conditions, as well as during the progression of injury and recovery following acute and chronic CNS injury.

## Funding

The author(s) disclosed receipt of the following financial support for the research, authorship, and/or publication of this article: This work was supported by NIH R01 HL79278 (JMG), NIH P01 NS32636 (JMG), NIH P30 NS057105 (Alafi Neuroimaging Core, Washington University), American Heart Association 09POST2280507 and 14SDG18410020 (AMS), NIH NS088555 (AMS), The Haggerty Center for Brain Injury and Repair (UTSW; AMS), NIH R01 NS052632 (RSK), NIH P01 NS059560 (RSK), and The Spastic Paralysis Research Foundation of the Illinois-Eastern Iowa District of Kiwanis International (JMG). AMS was also supported by the Hope

Center for Neurological Disorders, Washington University School of Medicine.

### Acknowledgements

The authors would like to thank Dr. Charlene Supnet and Katie Poinsette for help with editing this manuscript, and Erin Shubel and Neha Methani for help with data acquisition. We would also like to thank Dr. Denise Ramirez and Lisha Ma in the Whole Brain Microscopy Facility (UTSW) for assistance in the histology.

### Declaration of conflicting interests

The author(s) declared no potential conflicts of interest with respect to the research, authorship, and/or publication of this article.

### Authors' contributions

RSK, JMG, UMS, and AMS designed the studies, interpreted data, and drafted the manuscript; UMS, SBO, RH, XK, RG, AP, EJP, and AMS executed experiments and analyzed data. All authors revised and approved the final submission.

### Supplementary material

Supplementary material for this paper can be found at <http://jcbfm.sagepub.com/content/by/supplemental-data>

### References

- Liesz A, Zhou W, Mracsko E, et al. Inhibition of lymphocyte trafficking shields the brain against deleterious neuroinflammation after stroke. *Brain* 2011; 134: 704–720.
- Gelderblom M, Leyboldt F, Steinbach K, et al. Temporal and spatial dynamics of cerebral immune cell accumulation in stroke. *Stroke* 2009; 40: 1849–1857.
- Kamel H and Iadecola C. Brain-immune interactions and ischemic stroke: clinical implications. *Arch Neurol* 2012; 69: 576–581.
- Kim CH. Chemokine-chemokine receptor network in immune cell trafficking. *Curr Drug Targets Immune Endocr Metabol Disord* 2004; 4: 343–361.
- Jaerve A and Muller HW. Chemokines in CNS injury and repair. *Cell Tissue Res* 2012; 349: 229–48.
- McCandless EE, Piccio L, Woerner BM, et al. Pathological expression of CXCL12 at the blood-brain barrier correlates with severity of multiple sclerosis. *Am J Pathol* 2008; 172: 799–808.
- McCandless EE, Wang Q, Woerner BM, et al. CXCL12 limits inflammation by localizing mononuclear infiltrates to the perivascular space during experimental autoimmune encephalomyelitis. *J Immunol* 2006; 177: 8053–8064.
- Cruz-Orengo L, Holman DW, Dorsey D, et al. CXCR7 influences leukocyte entry into the CNS parenchyma by controlling abluminal CXCL12 abundance during autoimmunity. *J Exp Med* 2011; 208: 327–339.
- Stevens SL, Vartanian KB and Stenzel-Poore MP. Reprogramming the response to stroke by preconditioning. *Stroke* 2014; 45: 2527–2531.
- Stowe AM, Altay T, Freie AB, et al. Repetitive hypoxia extends endogenous neurovascular protection for stroke. *Ann Neurol* 2011; 69: 975–985.
- Monson NL, Ortega SB, Ireland SJ, et al. Repetitive hypoxic preconditioning induces an immunosuppressed B cell phenotype during endogenous protection from stroke. *J Neuroinflammation* 2014; 11: 22.
- Ceradini DJ, Kulkarni AR, Callaghan MJ, et al. Progenitor cell trafficking is regulated by hypoxic gradients through HIF-1 induction of SDF-1. *Nat Med* 2004; 10: 858–864.
- Hatse S, Princen K, Bridger G, et al. Chemokine receptor inhibition by AMD3100 is strictly confined to CXCR4. *FEBS Lett* 2002; 527: 255–262.
- Schioppa T, Uranchimeg B, Saccani A, et al. Regulation of the chemokine receptor CXCR4 by hypoxia. *J Exp Med* 2003; 198: 1391–1402.
- Stumm RK, Rummel J, Junker V, et al. A dual role for the SDF-1/CXCR4 chemokine receptor system in adult brain: isoform-selective regulation of SDF-1 expression modulates CXCR4-dependent neuronal plasticity and cerebral leukocyte recruitment after focal ischemia. *J Neurosci* 2002; 22: 5865–5878.
- Walter HL, van der Maten G, Antunes AR, et al. Treatment with AMD3100 attenuates the microglial response and improves outcome after experimental stroke. *J Neuroinflammation* 2015; 12: 24.
- Ruscher K, Kuric E, Liu Y, et al. Inhibition of CXCL12 signaling attenuates the postischemic immune response and improves functional recovery after stroke. *J Cereb Blood Flow Metab* 2013; 33: 1225–1234.
- Huang J, Li Y, Tang Y, et al. CXCR4 Antagonist AMD3100 protects blood-brain barrier integrity and reduces inflammatory response after focal ischemia in mice. *Stroke* 2013; 44: 190–197.
- Bodhankar S, Chen Y, Vandembark AA, et al. Treatment of experimental stroke with IL-10-producing B-cells reduces infarct size and peripheral and CNS inflammation in wild-type B-cell-sufficient mice. *Metab Brain Dis* 2014; 29: 59–73.
- Bodhankar S, Chen Y, Vandembark AA, et al. IL-10-producing B-cells limit CNS inflammation and infarct volume in experimental stroke. *Metab Brain Dis* 2013; 28: 375–386.
- Weise G and Stoll G. Magnetic resonance imaging of blood brain/nerve barrier dysfunction and leukocyte infiltration: closely related or discordant? *Front Neurol* 2012; 3: 178.
- Chen ZL, Indyk JA, Bugge TH, et al. Neuronal death and blood-brain barrier breakdown after excitotoxic injury are independent processes. *J Neurosci* 1999; 19: 9813–9820.
- Kleinschnitz C, Schwab N, Kraft P, et al. Early detrimental T-cell effects in experimental cerebral ischemia are neither related to adaptive immunity nor thrombus formation. *Blood* 2010; 115: 3835–3842.
- Cruz-Orengo L, Daniels BP, Dorsey D, et al. Enhanced sphingosine-1-phosphate receptor 2 expression underlies female CNS autoimmunity susceptibility. *J Clin Invest* 2014; 124: 2571–2584.

25. Cruz-Orengo L, Chen YJ, Kim JH, et al. CXCR7 antagonism prevents axonal injury during experimental autoimmune encephalomyelitis as revealed by in vivo axial diffusivity. *J Neuroinflammation* 2011; 8: 170.
26. Schonemeier B, Schulz S, Hoell V, et al. Enhanced expression of the CXCL12/SDF-1 chemokine receptor CXCR7 after cerebral ischemia in the rat brain. *J Neuroimmunol* 2008; 198: 39–45.
27. Li Y, Huang J, He X, et al. Postacute stromal cell-derived factor-1 $\alpha$  expression promotes neurovascular recovery in ischemic mice. *Stroke* 2014; 45: 1822–1829.
28. Kobayashi K, Sato K, Kida T, et al. Stromal cell-derived factor-1 $\alpha$ /C-X-C chemokine receptor type 4 axis promotes endothelial cell barrier integrity via phosphoinositide 3-kinase and Rac1 activation. *Arterioscler Thromb Vasc Biol* 2014; 34: 1716–1722.
29. Kim JH, Choi KH, Jang YJ, et al. Electroacupuncture preconditioning reduces cerebral ischemic injury via BDNF and SDF-1 $\alpha$  in mice. *BMC Complement Altern Med* 2013; 13: 22.
30. Davidson SM, Selvaraj P, He D, et al. Remote ischaemic preconditioning involves signalling through the SDF-1 $\alpha$ /CXCR4 signalling axis. *Basic Res Cardiol* 2013; 108: 377.
31. Li M, Hale JS, Rich JN, et al. Chemokine CXCL12 in neurodegenerative diseases: an SOS signal for stem cell-based repair. *Trends Neurosci* 2012; 35: 619–628.
32. Shao H, Tan Y, Eton D, et al. Statin and stromal cell-derived factor-1 additively promote angiogenesis by enhancement of progenitor cells incorporation into new vessels. *Stem Cells* 2008; 26: 1376–1384.
33. Yamaguchi J, Kusano KF, Masuo O, et al. Stromal cell-derived factor-1 effects on ex vivo expanded endothelial progenitor cell recruitment for ischemic neovascularization. *Circulation* 2003; 107: 1322–1328.
34. Cui X, Chopp M, Zacharek A, et al. Chemokine, vascular and therapeutic effects of combination simvastatin and BMSC treatment of stroke. *Neurobiol Dis* 2009; 36: 35–41.
35. Cui X, Chen J, Zacharek A, et al. Nitric oxide donor up-regulation of SDF1/CXCR4 and Ang1/Tie2 promotes neuroblast cell migration after stroke. *J Neurosci Res* 2009; 87: 86–95.
36. Bogoslovsky T, Spatz M, Chaudhry A, et al. Stromal-derived factor-1 $\alpha$  correlates with circulating endothelial progenitor cells and with acute lesion volume in stroke patients. *Stroke* 2011; 42: 618–625.
37. Sobrino T, Perez-Mato M, Brea D, et al. Temporal profile of molecular signatures associated with circulating endothelial progenitor cells in human ischemic stroke. *J Neurosci Res* 2012; 90: 1788–1793.
38. Hiesinger W, Perez-Aguilar JM, Atluri P, et al. Computational protein design to reengineer stromal cell-derived factor-1 $\alpha$  generates an effective and translatable angiogenic polypeptide analog. *Circulation* 2011; 124: S18–S26.
39. Yoo J, Seo JJ, Eom JH, et al. Effects of stromal cell-derived factor 1 $\alpha$  delivered at different phases of transient focal ischemia in rats. *Neuroscience* 2012; 209: 171–186.
40. Maziarz RT, Nademanee AP, Micallef IN, et al. Plerixafor plus granulocyte colony-stimulating factor improves the mobilization of hematopoietic stem cells in patients with non-Hodgkin lymphoma and low circulating peripheral blood CD34 $^{+}$  cells. *Biol Blood Marrow Transplant* 2013; 19: 670–675.